Development 140, 4214-4225 (2013) doi:10.1242/dev.100479

Growth factor-mediated mesodermal cell guidance and skeletogenesis during sea urchin gastrulation

Ashrifia Adomako-Ankomah and Charles A. Ettensohn*

SUMMARY

Growth factor signaling pathways provide essential cues to mesoderm cells during gastrulation in many metazoans. Recent studies have implicated the VEGF and FGF pathways in providing guidance and differentiation cues to primary mesenchyme cells (PMCs) during sea urchin gastrulation, although the relative contributions of these pathways and the cell behaviors they regulate are not fully understood. Here, we show that FGF and VEGF ligands are expressed in distinct domains in the embryonic ectoderm of *Lytechinus variegatus*. We find that PMC guidance is specifically disrupted in *Lv-vegf3* morphants and these embryos fail to form skeletal elements. By contrast, PMC migration is unaffected in *Lv-fgfa* morphants, and well-patterned but shortened skeletal elements form. We use a VEGFR inhibitor, axitinib, to show that VEGF signaling is essential not only for the initial phase of PMC migration (subequatorial ring formation), but also for the second phase (migration towards the animal pole). VEGF signaling is not required, however, for PMC fusion. Inhibition of VEGF signaling after the completion of PMC migration causes significant defects in skeletogenesis, selectively blocking the elongation of skeletal rods that support the larval arms, but not rods that form in the dorsal region of the embryo. Nanostring nCounter analysis of ~100 genes in the PMC gene regulatory network shows a decrease in the expression of many genes with proven or predicted roles in biomineralization in *vegf3* morphants. Our studies lead to a better understanding of the roles played by growth factors in sea urchin gastrulation and skeletogenesis.

KEY WORDS: Cell migration, Sea urchin, VEGF, FGF, Gastrulation, Primary mesenchyme cells

INTRODUCTION

Growth factor signaling pathways play essential roles in diverse developmental processes (Hogan, 1999; Wilson and Leptin, 2000; Wu and Hill, 2009; Dorey and Amaya, 2010), including the migration and differentiation of mesoderm cells during gastrulation. In *Drosophila* embryos, members of the fibroblast growth factor (FGF) family, *pyramus* and *thisbe*, are expressed in the ectoderm and regulate the intercalation, spreading, migration and differentiation of mesoderm cells, which express the FGF receptor *heartless* (Kadam et al., 2009; McMahon et al., 2010; Winklbauer and Müller, 2011; Reim et al., 2012). A similar role is played by platelet-derived growth factor (PDGF) during *Xenopus* gastrulation; in this case, the ligand PDGF-A, expressed in the ectoderm, regulates the orientation and migration of mesoderm cells that express PDGFRα (Ataliotis et al., 1995; Nagel et al., 2004; Damm and Winklbauer, 2011; Winklbauer and Müller, 2011). The migration of mesoderm cells away from the primitive streak in the gastrulating chick embryo is regulated by N-cadherin through the PDGF pathway (Yang et al., 2008; Chuai and Weijer, 2009), while FGF4 and FGF8 provide directional cues by acting as attractants and repellants, respectively (Yang et al., 2002; Lunn et al., 2007; Chuai and Weijer, 2009). Additionally, in the mouse embryo, FGF signaling regulates the migration of ingressed mesoderm cells and the formation of paraxial mesoderm (Sun et al., 1999; Ciruna and Rossant, 2001; Boulet and Capecchi, 2012).

The sea urchin embryo, which is optically clear and amenable to both cellular and molecular manipulations, serves as a valuable model with which to study the role of growth factors in gastrulation. Gastrulation in the sea urchin is characterized by the directional migration of mesodermal primary mesenchyme cells (PMCs), which produce the embryonic endoskeleton (Wilt and Ettensohn, 2007; Ettensohn, 2013). PMCs, after undergoing an epithelial-to-mesenchymal transition (EMT), migrate directionally within the blastocoel by means of filopodia and form a characteristic ring pattern (the subequatorial PMC ring), which consists of two ventrolateral clusters (VLCs) of PMCs joined by oral and aboral cell strands. The PMCs fuse as they migrate, forming a single continuous syncytium within which an elaborate calcium carbonate endoskeleton is secreted. Specific cues from the ectoderm of the embryo regulate both the migration and differentiation of the PMCs, thereby determining the structure of the resulting endoskeleton (Ettensohn and McClay, 1986; Ettensohn, 1990; Hardin et al., 1992; Armstrong et al., 1993; Ettensohn and Malinda, 1993; Guss and Ettensohn, 1997). However, relatively few genes expressed in the ectoderm have been shown to play a direct role in regulating PMC behavior (Di Bernardo et al., 1999; Cavalieri et al., 2003; Duloquin et al., 2007; Röttinger et al., 2008; Cavalieri et al., 2011).

Recent work has pointed to two pathways – mediated by vascular endothelial growth factor (VEGF) and FGF – in controlling the directional migration of PMCs and the formation of the embryonic skeleton (Duloquin et al., 2007; Röttinger et al., 2008). Duloquin et al. (Duloquin et al., 2007) showed that a VEGF receptor (VEGFR-10-Ig) is expressed selectively by migrating PMCs in the sea urchin *Paracentrotus lividus*, and a VEGF ligand (VEGF3) is expressed in the ectoderm overlying the VLCs. Perturbation of VEGF signaling in this species led to defects in PMC migration and skeletogenesis. Röttinger et al. (Röttinger et al., 2008) identified a similar, complementary pattern of expression of an FGF ligand and receptor (FGFA and FGFR2, respectively) in *P. lividus* and showed that blocking the FGF pathway also led to defects in skeletogenesis. These studies suggest that FGF and VEGF might have essential

Department of Biological Sciences, Carnegie Mellon University, Pittsburgh, PA 15213, USA.

*Author for correspondence (ettensohn@andrew.cmu.edu)

Accepted 30 July 2013

(and non-redundant) functions in mesoderm cell migration and skeletogenesis in the sea urchin, and raise the question of whether these two pathways regulate the same, or different, cell behaviors during PMC morphogenesis.

In this study, we aimed to further elucidate the roles of VEGF and FGF signaling in gastrulation and skeletogenesis in the sea urchin. We used two-color, fluorescent *in situ* hybridization to show that, in *Lytechinus variegatus*, *fgfa* and *vegf3* are expressed in distinct domains in the ectoderm. Knockdown of *Lv-vegf3* caused striking defects in the migration and differentiation of PMCs, whereas PMC migration was unperturbed in *Lv-fgfa* morphants, although these formed truncated skeletal elements. Using a second-generation VEGFR inhibitor, axitinib, we found that VEGF signaling is essential for all phases of PMC migration. Importantly, we identified a role for VEGF signaling in biomineralization that was separable from its effects on PMC migration, and showed that VEGF regulates the expression of many biomineralization genes in the PMC gene regulatory network (GRN). This study expands our knowledge of the regulation of mesoderm migration and differentiation by growth factor signaling pathways during gastrulation.

MATERIALS AND METHODS

Embryo culture

Adult *Lytechinus variegatus* were obtained from the Duke University Marine Laboratory (Beaufort, NC, USA) or Reeftopia (Key West, FL, USA). Adult *Strongylocentrotus purpuratus* were obtained from Pat Leahy (California Institute of Technology, Pasadena, CA, USA). Spawning was induced by intracoelomic injection of 0.5 M KCl and embryos were cultured in artificial seawater (ASW) at 23°C (*L. variegatus*) or 15°C (*S. purpuratus*).

Cloning of *Lv-vegf3*, *Lv-fgfa*, *Lv-otp* and *Lv-pax2/5/8*

Partial *Lv-fgfa* and *Lv-vegf3* sequences were obtained by PCR using degenerate primers (supplementary material Table S4). Remaining *Lv-vegf3* and 3′ *Lv-fgfa* sequences were obtained by RACE using *L. variegatus* late gastrula cDNA, the GeneRacer Kit with SuperScript III reverse transcriptase, and the Zero Blunt TOPO PCR Cloning Kit for Sequencing (Invitrogen). 5′ *Lv-fgfa* sequence was obtained by screening an *L. variegatus* mid-gastrula cDNA library (a gift from Dr David McClay, Duke University, NC, USA) using partial sequence obtained from degenerate PCR as a probe. GenBank accession numbers for *Lv-fgfa* and *Lv-vegf3* are KF285451 and KF285452, respectively. Comparisons of the sequences of *L. variegatus*, *S. purpuratus* and *Paracentrotus lividus* VEGF3 and FGFA were carried out using ClustalW (Thompson et al., 1994). A fragment of *Lv-pax2/5/8* and the complete *Lv-otp* coding region were obtained by PCR and cloned into the pCS2+ vector using the *Eco*RI and *Xba*I restriction sites.

Whole-mount *in situ* hybridization (WMISH)

Embryos were fixed (Adomako-Ankomah and Ettensohn, 2011) and WMISH and fluorescent WMISH (F-WMISH) were carried out (Lepage et al., 1992; Duloquin et al., 2007; Sharma and Ettensohn, 2010) as described.

Microinjection of morpholino antisense oligonucleotides (MOs)

Microinjections were carried out as described (Cheers and Ettensohn, 2004). Injection solutions contained 20% (vol/vol) glycerol and 0.16% (wt/vol) Texas Red dextran. MOs (supplementary material Table S5) were obtained from Gene Tools. *Lv-fgfa* splice-blocking MO was complementary to the exon 2/intron 2 boundary as described (Röttinger et al., 2008) and was injected at 2 mM and 4 mM. *Lv-fgfa* translation-blocking MO was injected at 4 mM and *Lv-vegf3* and *Sp-vegf3* translation-blocking MOs were injected at 2 mM.

RT-PCR analysis

RT-PCR analysis was performed as previously described (Adomako-Ankomah and Ettensohn, 2011). PCR products were cloned into the pCR4-TOPO vector (Invitrogen) for sequencing.

Axitinib (AG013736) treatments

A 5 mM stock solution of axitinib (Selleckchem, Houston, TX, USA) was prepared in DMSO and stored at −20°C. Embryos were cultured in ASW containing axitinib at a final concentration of 75 nM (*L. variegatus*) or 50 nM (*S. purpuratus*). Control embryos were cultured in equivalent concentrations of DMSO.

Immunofluorescence

Immunofluorescence using monoclonal antibody (mAb) 6a9 was carried out as described (Ettensohn and McClay, 1988). Immunostained embryos were examined using a Zeiss LSM 510 Meta/UV DuoScan inverted spectral confocal microscope.

Apoptosis assay

The terminal dUTP nick end labeling (TUNEL) assay was carried out using the ApoAlert DNA Fragmentation Assay Kit (Clontech) as described (Voronina and Wessel, 2001). Modifications were introduced to label PMCs with the 6e10 mAb (Hodor et al., 2000), prior to nuclear labeling with 0.2 mg/ml Hoechst stain. Embryos were observed by confocal microscopy as described above.

Analysis of PMC migration and filopodia extension

To assess the ability of PMCs in axitinib- and DMSO-treated (control) embryos to target to the vegetal region of the embryo, PMCs were scattered throughout the blastocoel at the mesenchyme blastula stage (prior to the invagination of the archenteron) using a microneedle (Ettensohn and McClay, 1988). Embryos were cultured at 23°C for 5 hours, then fixed in 4% paraformaldehyde (1 hour), washed twice in ASW, and post-fixed in 100% methanol (20 minutes). The distribution of PMCs in the blastocoel was assayed by 6a9 immunostaining.

To further analyze PMC migration, PMCs were removed microsurgically from late mesenchyme blastula stage embryos and placed on fibronectin-coated coverslips as described (Malinda et al., 1995) in a medium of 2% horse serum in ASW. After allowing 30 minutes for attachment, PMCs from DMSO- or axitinib-treated embryos were imaged at 5-minute intervals for 2.5 hours using an Olympus DP71 digital camera. The velocity of migrating PMCs was measured using the Manual Tracking plug-in of ImageJ (NIH). Individual PMCs were tracked either throughout the experiment or until they became untraceable due to clustering.

To quantify filopodial numbers and lengths in axitinib- and DMSO-treated embryos, PMCs were scattered in the blastocoel at the mesenchyme blastula stage, and approximately half of the cells were flushed out of the blastocoel to reduce cell density. This made it possible to visualize unambiguously the filopodia of individual PMCs. Embryos were cultured at 23°C for 1.5 hours post-surgery, and the distribution and length of filopodia present were measured in 6a9-stained embryos using ImageJ.

PMC fusion assay

PMC fusion was monitored by dye transfer (Hodor and Ettensohn, 2008). One set of fertilized eggs was injected with a solution of *Lv-vegf3* MO that contained 10% (wt/vol) fluorescein dextran, while another set was injected with a solution of the same MO without the dextran. At the mesenchyme blastula stage, two to six PMCs were transferred from dextran-labeled donor embryos into each unlabeled host embryo. Embryos were observed by confocal microscopy 6 and 24 hours post-surgery to assess the distribution of the dextran within the PMC syncytium.

Assay of gene expression using the Nanostring nCounter analysis system

Changes in mRNA levels were assayed using the Nanostring nCounter analysis system (Nanostring Technologies, Seattle, WA, USA) (Geiss et al., 2008). For each experiment, RNA was extracted from 200 control and 200 axitinib-treated or VEGF morphant *S. purpuratus* embryos using the Nucleospin RNA II Kit (Clontech). The code set of probes corresponded to ~80 genes in the PMC GRN (supplementary material Table S2).

RESULTS

VEGF and FGF ligands are expressed in distinct domains in the ectoderm

To compare the roles of VEGF and FGF signaling, we cloned *vegf3* and *fgfa* from *L. variegatus*, a North American species. ClustalW analysis (Thompson et al., 1994) of the amino acid sequences of VEGF3 and FGFA in *L. variegatus*, *S. purpuratus* and *P. lividus* revealed ~70% and 80% identity, respectively, across species (supplementary material Fig. S1).

We performed two-color F-WMISH to compare directly the expression domains of *Lv-fgfa* and *Lv-vegf3* at various developmental stages (Fig. 1). *Lv-fgfa* showed a highly dynamic pattern of expression whereas *Lv-vegf3* expression was steadily maintained in ectodermal territories associated with PMC accumulation and skeletal growth. Both genes were first detectable at the hatched blastula stage (Fig. 1A-A‴), when *Lv-fgfa* was expressed in a ring of ectoderm that spanned the equator of the embryo and in the presumptive PMCs at the vegetal pole. *Lv-vegf3* was also expressed in a ring in the ectoderm, but in a territory more vegetal to, and not overlapping with, the domain of *Lv-fgfa* expression. This separation of expression domains persisted at the mesenchyme blastula stage, although at this stage the expression of both genes was generally restricted to the ectoderm overlying the VLCs (Fig. 1B-B‴). As the archenteron began to invaginate, the expression domains of *Lv-fgfa* and *Lv-vegf3* in the ectoderm overlapped slightly (Fig. 1C-C‴). This overlap persisted as the archenteron elongated (Fig. 1D-D‴), but was no longer evident at the late gastrula stage (Fig. 1E-E‴), when *Lv-vegf3* continued to be expressed in the ectoderm overlying the VLCs (Fig. 1E′) while *Lv-fgfa* was downregulated in these domains and was expressed mostly in two apical domains of ectoderm and in PMCs (Fig. 1E). *Lv-fgfa* expression at the prism stage was largely restricted to the PMCs, whereas *Lv-vegf3* expression persisted in the ectoderm adjacent to these cells (Fig. 1F-F‴). At the pluteus stage, *Lv-vegf3* was expressed in the ectoderm at specific regions overlying the elongating postoral and anterolateral rods, while *Lv-fgfa* was expressed in PMCs associated with these rods and in the gut (Fig. 1G-G‴). Additionally, we observed that the cognate receptors *Lv-vegfr-10-Ig* and *Lv-fgfr-2* were expressed selectively by PMCs in patterns identical to those reported in *P. lividus* (Duloquin et al., 2007; Röttinger et al., 2008) (data not shown).

VEGF signaling plays a more prominent role than FGF signaling in PMC migration and skeletogenesis in *L. variegatus*

To compare the functions of FGF and VEGF in *L. variegatus*, we knocked down the expression of each ligand. Skeletogenesis was blocked in embryos injected with 2 mM *Lv-vegf3* translation-blocking MO (Fig. 2A-B′), a phenotype very similar to that observed in *P. lividus* (Duloquin et al., 2007). Likewise,

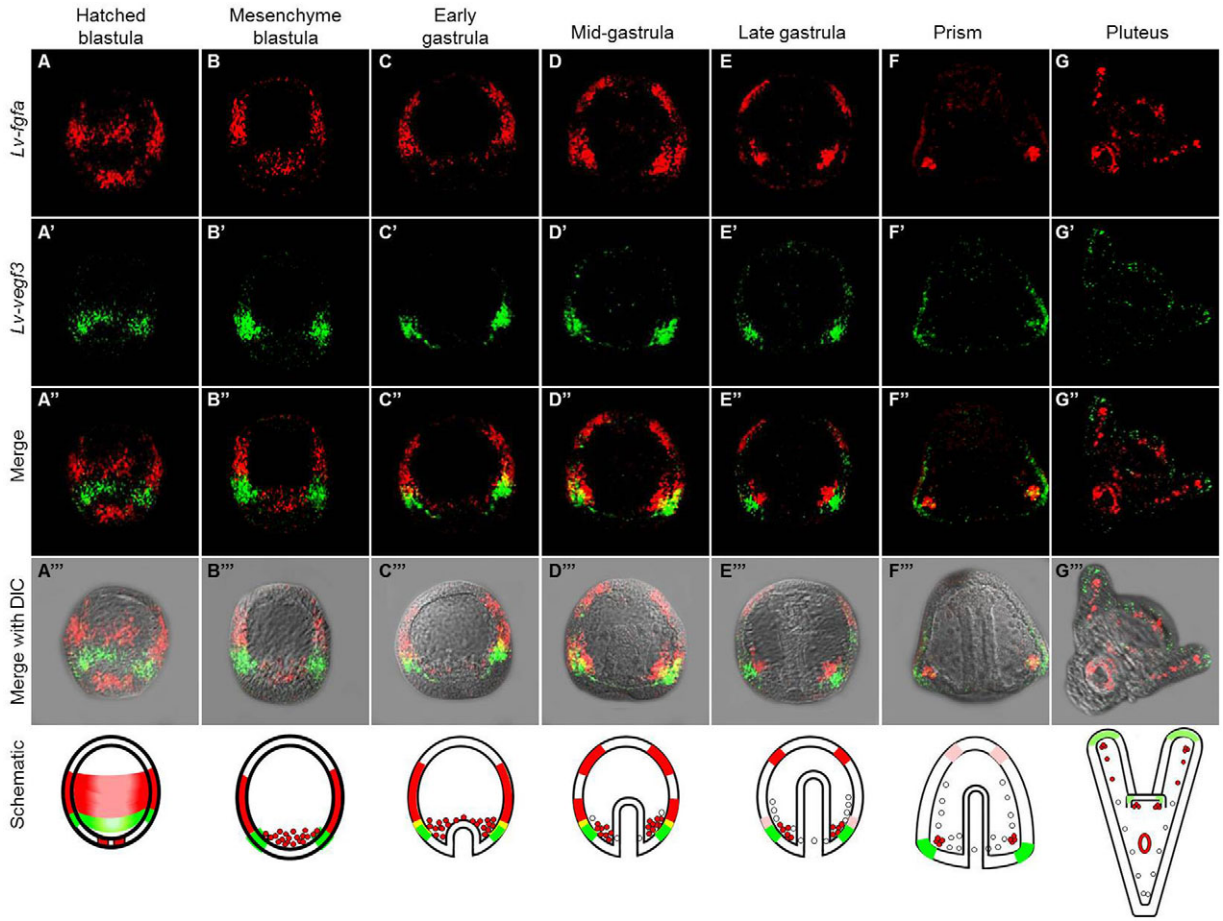

Fig. 1. FGF and VEGF ligands are expressed in mostly independent domains in the sea urchin ectoderm. F-WMISH analysis of *Lv-fgfa* (A-G) and *Lv-vegf3* (A′-G′) expression shows that their expression domains are entirely separate at hatched blastula (**A-A‴**) and mesenchyme blastula (**B-B‴**) stages. Their expression domains overlap at early gastrula (**C-C‴**) and mid-gastrula (**D-D‴**) stages. At late gastrula (**E-E‴**), prism (**F-F‴**) and pluteus (**G-G‴**) stages, *Lv-fgfa* and *Lv-vegf3* are once again expressed in independent domains. Schematics beneath illustrate the expression patterns.

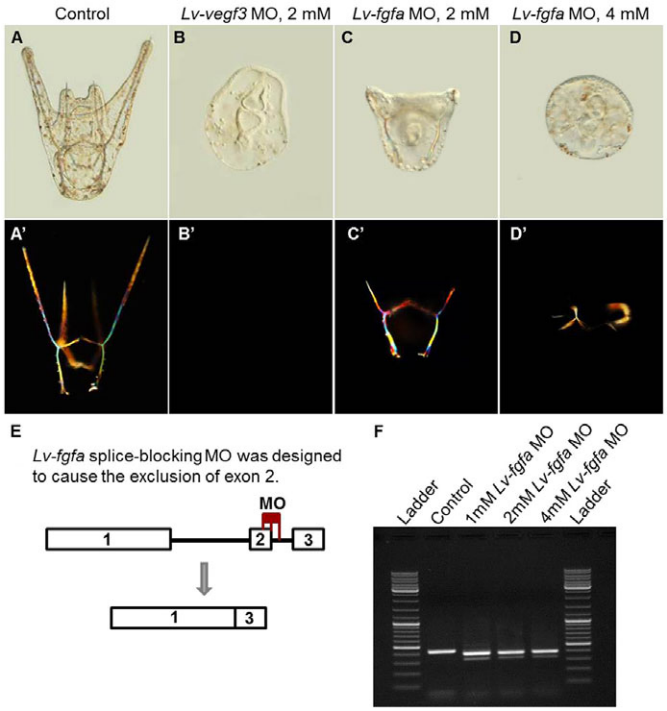

Fig. 2. Knockdown of *Lv-vegf3*, but not *Lv-fgfa*, blocks skeletogenesis. (**A-D′**) DIC (A-D) and polarized light (A′-D′) images of a control embryo (A,A′), an embryo injected with 2 mM *Lv-vegf3* translation-blocking MO (B,B′), and embryos injected with 2 mM (C,C′) and 4 mM (D,D′) *Lv-fgfa* splice-blocking MO. No skeletal elements form in *Lv-vegf3* morphants (99% of embryos scored, *n*=200), but shortened skeletal elements form in *Lv-fgfa* morphants (90% of embryos scored, *n*=200). (**E**) Design of the *Lv-fgfa* splice-blocking MO. (**F**) Agarose gel showing shift in size of the *Lv-fgfa* transcript in MO-injected embryos. The bright band in morphant samples was sequenced and lacked exon 2. Ladder, Fermentas GeneRuler DNA Ladder mix.

skeletogenesis was eliminated in *S. purpuratus* embryos injected with 2 mM *Sp-vegf3* translation-blocking MO (supplementary material Fig. S2B,B′). The *Lv-vegf3* and *Sp-vegf3* MOs differed at 8/25 nucleotide positions, demonstrating the specificity of the morphant phenotype. However, unlike results obtained in *P. lividus* (Röttinger et al., 2008), skeletogenesis was not eliminated in embryos injected with 2 mM splice-blocking *Lv-fgfa* MO, and these morphants formed extensive, although truncated, skeletons (Fig. 2C,C′). Embryos injected with as much as 4 mM *Lv-fgfa* MO also formed skeletal elements (Fig. 2D′), although these embryos showed toxicity effects due to the high MO concentration (Fig. 2D).

Following the same splice-blocking strategy used by Röttinger et al. (Röttinger et al., 2008), we designed the *Lv-fgfa* MO to overlap the exon 2-intron 2 boundary, leading to the exclusion of exon 2, which contains the highly conserved FGF domain (Fig. 2E). We demonstrated the effectiveness of the MO by RT-PCR analysis of 200 control embryos and 200 embryos injected with 1, 2 or 4 mM *Lv-fgfa* MO and observed the expected shift in the size of the *Lv-fgfa* transcript corresponding to an exclusion of exon 2 in embryos injected with all concentrations of *Lv-fgfa* MO (Fig. 2F, bright bands). At the MO concentrations used in our subsequent analysis (2 mM), we did not detect normally spliced *Lv-fgfa* mRNA by RT-PCR. The structure of the mis-spliced form of the mRNA lacking exon 2 was confirmed by sequencing. Embryos injected with an *Lv-fgfa* translation-blocking MO at a range of concentrations likewise formed bilaterally symmetrical, truncated skeletal elements (supplementary material Fig. S3B,D).

We examined the distribution of PMCs in *Lv-vegf3* and *Lv-fgfa* morphants by 6a9 immunostaining. At the late gastrula stage, PMCs in control embryos were arranged in a subequatorial ring with VLCs (Fig. 3A, arrow). PMCs in *Lv-vegf3* morphants did not form VLCs (Fig. 3B,B′), although most of the cells remained localized in the vegetal hemisphere. By contrast, PMCs in *Lv-fgfa* morphants formed a well-patterned ring comparable to that of control embryos (Fig. 3C,C′). At the pluteus stage, PMCs in control embryos were aligned along a well-developed skeleton (Fig. 3D,D′), whereas PMCs in *Lv-vegf3* morphants were scattered primarily within the vegetal region of the embryo (Fig. 3E,E′). Strikingly, in *Lv-vegf3* morphants, PMCs were highly fragmented at the pluteus stage (Fig. 3E, inset), but not at earlier stages (Fig. 3B, inset). We showed by a TUNEL assay that this fragmentation was not due to apoptosis (supplementary material Fig. S4). In *Lv-fgfa* morphants at the pluteus stage, PMCs were arranged in a pattern similar to that observed in control embryos, although defects in the morphology of the skeleton were apparent (Fig. 3F,F′).

We tested whether signaling through the VEGF and FGF pathways regulated the expression of *Lv-vegf3* or *Lv-fgfa*. *Lv-vegf3* expression was strongly upregulated in *Lv-vegf3* morphants (Fig. 4A,B). We also observed a striking downregulation of *Lv-fgfa* in PMCs, from the mesenchyme blastula stage throughout later development (Fig. 4C,D). *Lv-fgfa* was expressed in an expanded territory in the ectoderm at the late gastrula stage in *Lv-vegf3* morphants (Fig. 4D), although this expression domain narrowed to a pattern comparable to that of controls by the prism stage (data not shown). Upon *Lv-fgfa* knockdown, *Lv-vegf3* was slightly upregulated, an effect that was more pronounced at mesenchyme blastula (Fig. 4E) than at late gastrula (Fig. 4F) stages. Furthermore, as previously described in *P. lividus* (Röttinger et al., 2008), *Lv-fgfa* expression was strongly upregulated in the PMCs and ectoderm of *Lv-fgfa* morphants (Fig. 4G,H). The increase in *Lv-vegf3* and *Lv-fgfa* mRNA levels in the corresponding morphants is likely to reflect negative feedback of each pathway on transcription, although we cannot exclude the possibility that mRNA stability is affected (directly or indirectly) by the MOs.

We also examined two other genes expressed in the ectoderm that have been shown to play a role in regulating skeletogenesis: *otp* (Di Bernardo et al., 1999; Cavalieri et al., 2003) and *pax2/5/8* (Cavalieri et al., 2011). *Lv-pax2/5/8* expression was slightly downregulated in *Lv-vegf3* morphants (supplementary material Fig. S5A,A′) and strongly downregulated in *Lv-fgfa* morphants (supplementary material Fig. S5C,C′). *Lv-otp* was unaffected by the knockdown of either *Lv-vegf3* or *Lv-fgfa* (supplementary material Fig. S5B,B′,D,D′). As *Lv-fgfa* knockdown produced only modest defects in skeletogenesis and had no detectable effect on PMC migration, we focused our attention on further elucidating the role of VEGF signaling in PMC morphogenesis.

VEGF signaling controls PMC pathfinding throughout gastrulation

VEGF MO injection blocks VEGF signaling throughout embryogenesis. To determine the temporal requirements for VEGF signaling, we used a second-generation VEGFR inhibitor, axitinib, which specifically blocks VEGF signaling at low (nM) concentrations (Hu-Lowe et al., 2008; Bhargava and Robinson, 2011). *L. variegatus* embryos cultured in 75 nM axitinib from early cleavage developed no skeletal elements (Fig. 5B,B′), a phenotype identical to that of VEGF morphants (Fig. 2B). As in *Lv-vegf3* morphants, PMCs in axitinib-

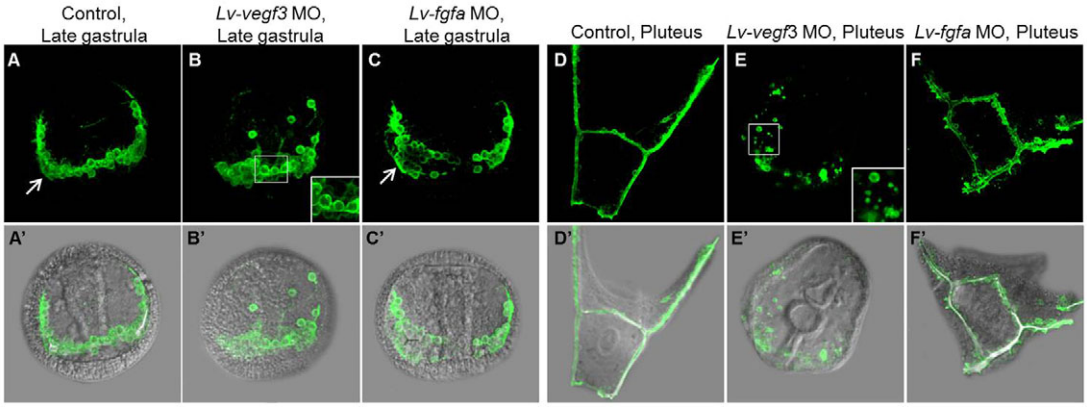

Fig. 3. PMC migration is perturbed in *Lv-vegf3*, but not *Lv-fgfa*, morphants. Fluorescence (A-F) and DIC-merged (A′-F′) images of control embryos (**A**,**A′**,**D**,**D′**), *Lv-vegf3* morphants (**B**,**B′**,**E**,**E′**) and *Lv-fgfa* morphants (**C**,**C′**,**F**,**F′**) at late gastrula (A-C) and pluteus (D-F) stages. 6a9 immunostaining shows that directed PMC migration is disrupted in *Lv-vegf3* morphants but unperturbed in *Lv-fgfa* morphants. In *Lv-vegf3* morphants, PMCs appear fragmented at the pluteus stage (E, inset) compared with the late gastrula stage (B, inset). Arrows indicate well-formed VLCs at the late gastrula stage in control (A) and *Lv-fgfa* morphant (C) embryos.

treated embryos did not form VLCs (Fig. 5D,D′). At the pluteus stage, PMCs in axitinib-treated embryos exhibited the same fragmented phenotype observed in *Lv-vegf3* morphants (Fig. 5F). Similarly, PMC migration and skeletogenesis were inhibited in *S. purpuratus* embryos cultured in 50 nM axitinib from early cleavage (supplementary material Fig. S2C,C′,F,F′). These findings confirmed that axitinib phenocopies VEGF knockdown.

PMC migration can be considered to occur in two phases. During the initial phase (early gastrulation), PMCs disperse from the site of ingression and arrange themselves in the subequatorial ring. During the second phase (late gastrulation), a chain of PMCs migrates from each VLC towards the animal pole. These cells produce the dorsoventral, anterolateral, and recurrent rods of the larval skeleton. To test whether VEGF signaling is required for the second phase of PMC migration, we cultured embryos in axitinib from the early gastrula stage, when PMCs were in the process of forming the subequatorial ring (Fig. 6A,A′). We fixed control and axitinib-treated embryos at the late gastrula stage and assessed the distribution of PMCs by immunostaining. PMCs in DMSO-treated control embryos migrated normally and formed two chains of cells that extended from the VLCs towards the animal pole (Fig. 6C,C′). No strands of PMCs migrated towards the animal pole in axitinib-treated embryos, however, despite the fact that VLCs were visible in 80% of embryos (Fig. 6B,B′). Based on these observations, we conclude that VEGF signaling is required for both the early and late phases of PMC migration.

Upon *Lv-vegf3* knockdown or VEGFR inhibition by axitinib treatment, PMCs did not disperse randomly through the blastocoel but remained mostly in the vegetal hemisphere. To examine whether this behavior might be the result of VEGF-independent guidance cues in the blastocoel, we displaced PMCs throughout the blastocoel in control (Fig. 7A,A′) and axitinib-treated embryos at the mesenchyme blastula stage and examined the distribution of PMCs 5 hours later. In 28/30 cases, PMCs in control embryos returned to the vegetal region

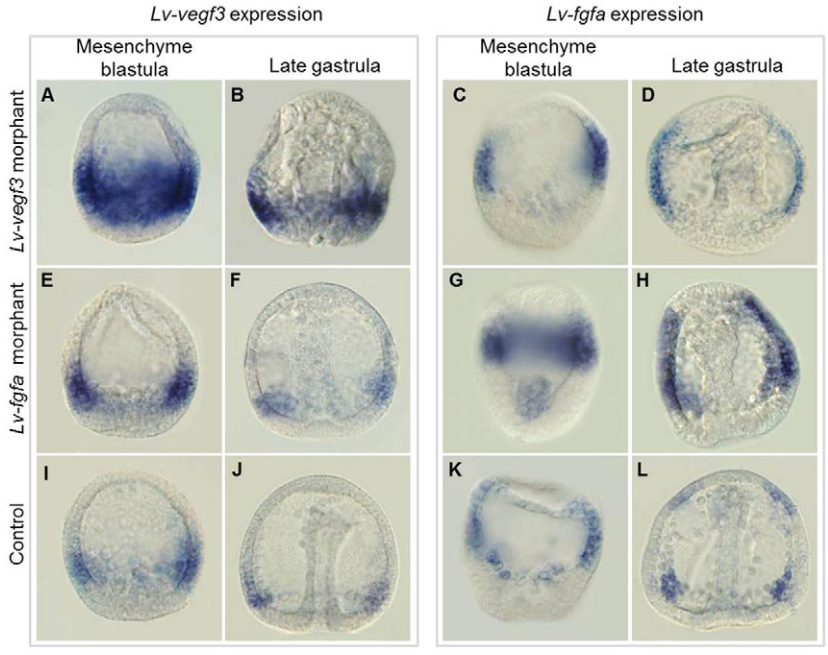

Fig. 4. Complex interactions between VEGF and FGF signaling and expression of *Lv-vegf3* and *Lv-fgfa*. WMISH analysis of *Lv-vegf3* (**A**,**B**,**E**,**F**,**I**,**J**) and *Lv-fgfa* (**C**,**D**,**G**,**H**,**K**,**L**) expression in *Lv-vegf3* morphants (A-D), *Lv-fgfa* morphants (E-H) and controls (I-L) at the mesenchyme blastula (A,C,E,G,I, K) and late gastrula (B,D,F,H,J,L) stages. In *Lv-vegf3* morphants, *Lv-vegf3* is strongly upregulated (A,B), whereas *Lv-fgfa* is downregulated in the PMCs and upregulated in the ectoderm (C,D). In *Lv-fgfa* morphants, *Lv-vegf3* expression is slightly upregulated (E,F), whereas *Lv-fgfa* is strongly upregulated both in the PMCs and in the ectoderm (G,H).

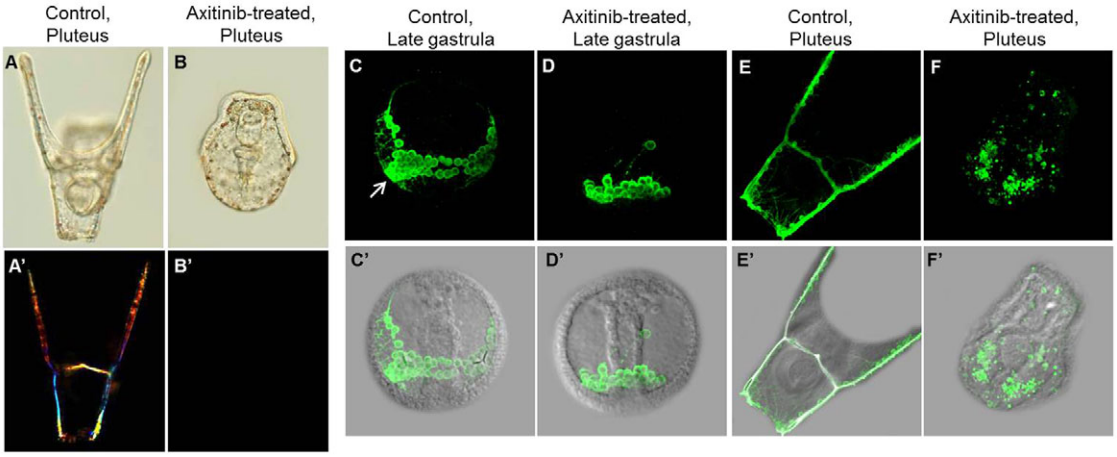

Fig. 5. VEGFR inhibition with axitinib phenocopies *Lv-vegf3* morphants. (**A-B′**) DIC (A,B) and polarized light (A′,B′) images of a control embryo (A,A′) and an embryo treated with 75 mM axitinib from the 2-cell stage (B,B′) show that axitinib inhibits skeletogenesis. (**C-F′**) Fluorescence (C-F) and DIC-merged (C′-F′) images of control (C,C′,E,E′) and axitinib-treated (D,D′,F,F′) embryos at late gastrula (C-D′) and pluteus (E-F′) stages (6a9 immunostaining), demonstrate that PMC migration is perturbed by axitinib. Arrow (C) indicates well-formed VLC in control embryo.

and formed a subequatorial ring, usually with two chains of cells extending towards the animal pole (Fig. 7C,C′). By contrast, in 30/30 axitinib-treated embryos, many PMCs remained in the animal half of the embryo (Fig. 7B,B′). Comparable results were obtained when PMCs in *Lv-vegf3* morphants were scattered in the same manner (data not shown). Aggregates of PMCs remained scattered throughout the blastocoel of axitinib-treated embryos even 10 hours post-surgery (Fig. 7D,D′), whereas extensive, well-patterned skeletal elements were visible in control embryos (Fig. 7E,E′). We therefore found no evidence of a VEGF-independent mechanism that targets PMCs to the vegetal hemisphere.

VEGF signaling is not required for PMC motility per se or for PMC fusion, but regulates the number and length of filopodia

In axitinib-treated embryos and *Lv-vegf3* morphants, PMCs dispersed from the site of ingression and migrated along the basal surface of the ectoderm, indicating that cell motility per se was not blocked. We also used an *in vitro* assay to examine PMC motility (Fig. 8). Control PMCs migrated actively on fibronectin-coated coverslips and formed aggregates, as did PMCs that were isolated from axitinib-treated embryos and cultured continuously in the presence of the inhibitor (Fig. 8A). Axitinib treatment resulted in a very small, statistically insignificant decrease in average PMC velocity (P=0.1298) (Fig. 8B). These results support the view that VEGF signaling has a specific role in PMC guidance but is not required for PMC motility.

Because PMC pathfinding is likely to be mediated by filopodia, we analyzed the effect of VEGF signaling on the number and length of filopodia. PMCs in control embryos showed a stereotypical elongated morphology with filopodia that extended mostly from the two ends of each cell (Fig. 9A). PMCs in axitinib-treated embryos, however, were more rounded and had fewer, shorter filopodia (Fig. 9B). PMCs in control embryos (n=57) had ~5 filopodia per cell, of an average length of 11.5 μm. By contrast, PMCs in axitinib-treated embryos (n=63) had ~2 filopodia per cell, of an average length of 4.8 μm (Fig. 9C,D). These differences between control and axitinib-treated embryos were highly significant ($P=7.68\times10^{-8}$ and $P=5.15\times10^{-29}$ for filopodia number and length, respectively). These findings strongly suggest that VEGF signaling regulates aspects of filopodial dynamics, i.e. the formation of these cell protrusions and/or their stability.

Filopodia also mediate PMC-PMC fusion (Hodor and Ettensohn, 2008). We used a dye-transfer assay to test whether PMC fusion was blocked in *Lv-vegf3* morphants. In 20/21 morphant embryos, dextran spread from a small number of transplanted, labeled PMCs to all host PMCs by the late gastrula stage (Fig. 10A,A′), demonstrating that PMC fusion occurred. At the pluteus stage, the dextran label was still visible in the fragmented PMCs of *Lv-vegf3* morphant embryos (Fig. 10B,B′).

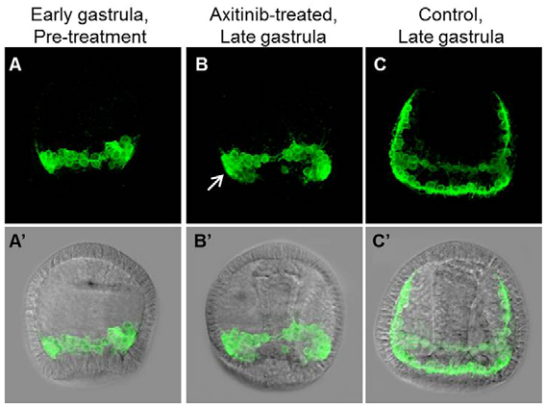

Fig. 6. VEGF signaling regulates late stages of PMC migration. Fluorescence (A-C) and DIC-merged (A′-C′) images of early gastrula embryos immediately prior to axitinib treatment (**A**,**A′**), late gastrula embryos treated with axitinib from the early gastrula stage (**B**,**B′**) and control late gastrula embryos treated with DMSO from the early gastrula stage (**C**,**C′**) (6a9 immunostaining). PMC migration towards the animal pole is inhibited by axitinib. Arrow (B) indicates VLC.

VEGF signaling is required continuously for skeletogenesis

Why do PMCs fail to produce skeletal elements when VEGF signaling is blocked? One possibility is that VEGF regulates biomineralization directly, by regulating the expression of biomineralization genes. Alternatively, VEGF might regulate

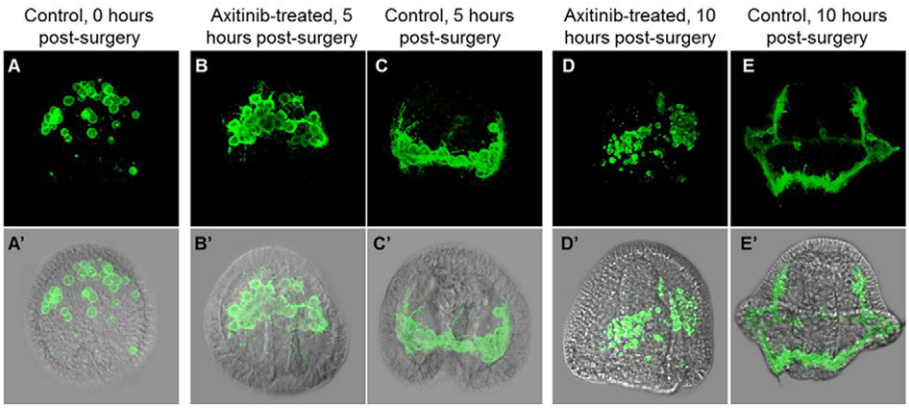

Fig. 7. VEGF signaling is required for the targeting of PMCs to the vegetal hemisphere. At the mesenchyme blastula stage, a micropipette was used to scatter PMCs, redistributing most of the cells into the animal hemisphere. Fluorescence (**A-E**), and DIC-merged (**A′-E′**) images of a control embryo 0 hours post-surgery (A,A′), and axitinib-treated (B,B′,D,D′) and DMSO-treated control (C,C′,E,E′) embryos 5 hours (B,B′,C,C′) and 10 hours (D,D′,E,E′) after surgery. At 5 hours, almost all PMCs have migrated to the vegetal hemisphere and have formed a subequatorial ring in control embryos, whereas in axitinib-treated embryos most PMCs remain in the animal hemisphere. At 10 hours, a well-patterned skeleton is visible in control embryos, whereas PMCs in axitinib-treated embryos are aggregated within the blastocoel.

biomineralization indirectly, by affecting the ability of PMCs to migrate directionally and accumulate in the VLCs, where local ectodermal cues other than VEGF might induce biomineral secretion. To distinguish between these possibilities, we treated embryo cultures with axitinib at various stages of development (Fig. 11). The frequencies of morphant phenotypes that we observed upon drug addition at each stage of development are shown in Table 1. Embryos treated with axitinib beginning at the hatched blastula (Fig. 11B,B′), mesenchyme blastula (Fig. 11C,C′) or early gastrula (Fig. 11D,D′) stages developed no skeletal elements when control embryos reached the pluteus stage (Fig. 11A,A′). Embryos treated with axitinib from the mid-gastrula (Fig. 10E,E′), late gastrula (Fig. 11F,F′) or prism (Fig. 11G,G′) stages developed truncated skeletal elements.

Surprisingly, we noted that in embryos cultured in axitinib from the mid- or late gastrula stages, specific skeletal rods were affected to varying degrees. The body rods and recurrent rods extended

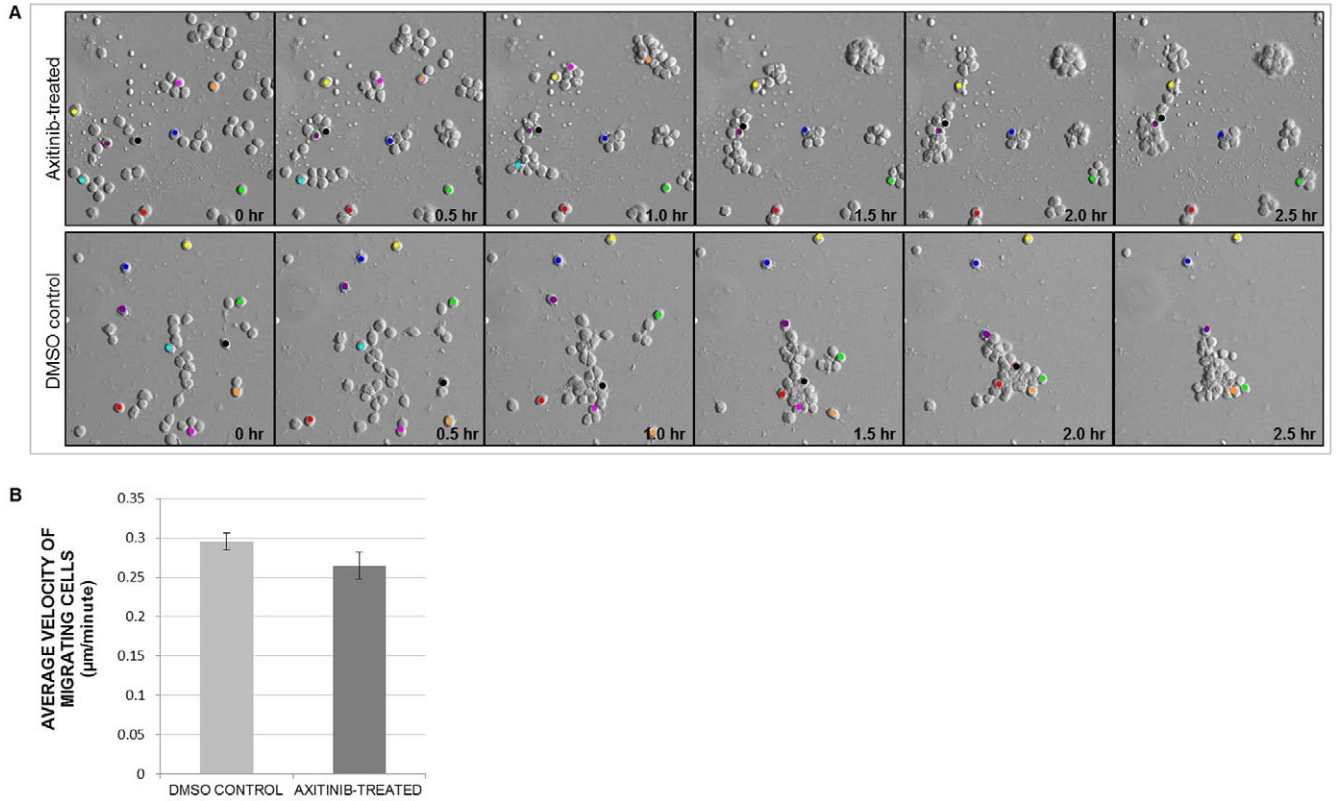

Fig. 8. VEGF signaling is not required for PMC translocation *in vitro*. (**A**) DIC images of PMCs treated with DMSO (control) or axitinib show that PMC motility and cell clustering on fibronectin-coated coverslips are not perturbed when VEGF signaling is blocked. (**B**) The average velocities of migrating control (n=223) and axitinib-treated (n=200) PMCs are not statistically different (P=0.1298). Error bars indicate s.e.m.

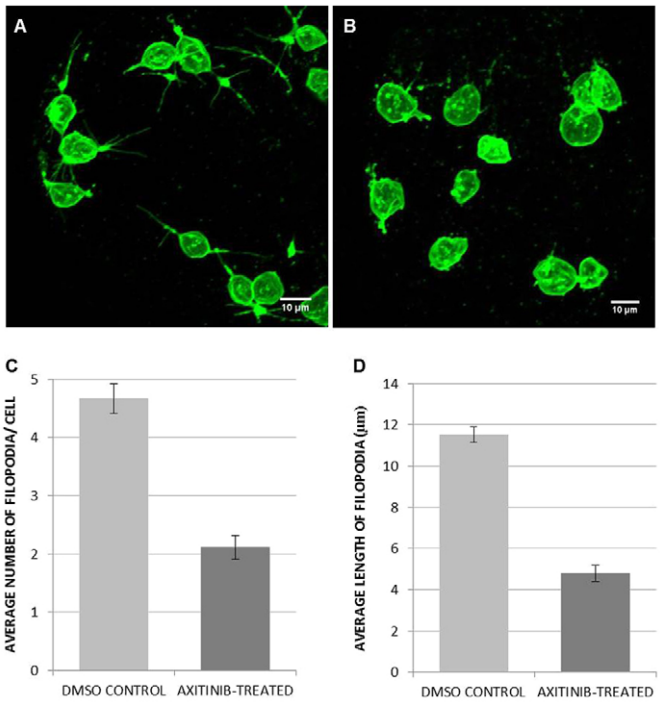

Fig. 9. VEGF signaling regulates the number and length of PMC filopodia. (**A**,**B**) Fluorescence images of control (A) and axitinib-treated (B) embryos 1.5 hours after PMCs were scattered within the blastocoel. PMCs in control embryos extend more filopodia than PMCs in axitinib-treated embryos and these filopodia are longer in controls. (**C**,**D**) The average number of filopodia per cell (C) and the average length of filopodia (D) extended by PMCs in control embryos (*n*=57) and axitinib-treated embryos (*n*=63). Error bars indicate s.e.m.

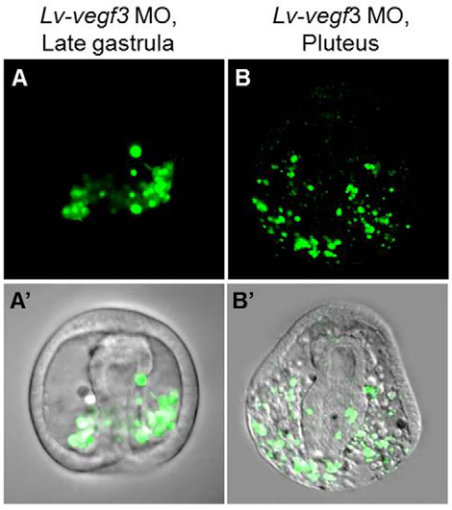

Fig. 10. VEGF signaling does not regulate PMC fusion. Fluorescence (**A**,**B**), and DIC-merged (**A′**,**B′**) images of *Lv-vegf3* morphant hosts 6 hours (A,A′) and 24 hours (B,B′) after a few FITC-dextran labeled PMCs were transferred from *Lv-vegf3* morphant donors. PMCs are fusion competent, as shown by the spread of dextran throughout the syncytium 6 hours post-surgery (A) and in scattered fragmented PMCs 24 hour post-surgery (B).

normally in the dorsal region of the embryo (Fig. 11E′,F′, arrows, Fig. 12) whereas the postoral and anterolateral rods were severely truncated (Fig. 12). The postoral and anterolateral rods grow via the activity of a plug of PMCs at their tips; these PMC clusters were apparent in axitinib-treated embryos, although the rods failed to elongate normally (supplementary material Fig. S6).

We also examined the reversibility of the effects of VEGF inhibition on skeletogenesis. Embryos were cultured in axitinib from early cleavage and the inhibitor was washed out at various stages of development (supplementary material Fig. S7). Most embryos recovered fully from the effects of blocking VEGF signaling if axitinib was removed prior to the end of gastrulation (supplementary material Fig. S7B′-E′, Table S1), whereas embryos cultured in axitinib post-gastrulation had limited, if any, ability to form skeletal elements after removal of the drug (supplementary material Fig. S7F-H′, Table S1).

VEGF signaling regulates the expression of genes in the PMC GRN

Because VEGF signaling regulates biomineralization directly (Figs 11, 12), we tested the role of this pathway in regulating the expression of genes in the PMC GRN. *S. purpuratus* embryos were used because the availability of a sequenced genome facilitated the design of a Nanostring probe set (supplementary material Table S2). Blocking VEGF signaling in *S. purpuratus* either with an *Sp-vegf3* translation-blocking MO or by culturing embryos in 50 nM axitinib from early cleavage perturbed PMC migration and differentiation, as in *L. variegatus* (supplementary material Fig. S2). Differences in mRNA levels between control embryos and *Sp-vegf3* morphants or embryos cultured in axitinib from early cleavage were measured at the late gastrula stage (48 hours postfertilization) (supplementary material Table S3). Three independent trials were conducted for both *Sp-vegf3* morphants and axitinib-treated embryos.

We found that 19/90 genes (21%) showed a change in expression of greater than 50% in *Sp-vegf3* morphants, the great majority of which were effector genes with proven or predicted roles in biomineralization (Fig. 13A; supplementary material Table S3). Similar results were obtained with axitinib-treated embryos, in which 21/90 genes (23%) showed a change of 50% or more (Fig. 13B; supplementary material Table S3). Of all genes that showed a change in expression of 50% or more, 14 were common to both the MO and axitinib-treated samples (74% and 67% of the affected genes, respectively). Most regulatory genes showed little or no change in both sample sets, an observation which is consistent with the fact that VEGF signaling does not regulate PMC specification.

DISCUSSION

Growth factors play a crucial role in regulating mesoderm morphogenesis during gastrulation, but the specific growth factors involved and the cell behaviors they control vary across species. For example, in the chick embryo, mesoderm migration is regulated by a combination of signals (PDGF, FGF and VEGF) (Chuai and Weijer, 2009), whereas our results indicate that in the sea urchin [which lacks PDGF and PDGF receptor genes (Lapraz et al., 2006)] PMC migration is controlled predominantly by one growth factor (VEGF3). In several organisms, it has been shown that a single growth factor influences multiple cell behaviors, although the details vary. During *Xenopus* gastrulation, PDGF regulates the orientation, radial intercalation and directional migration of mesodermal cells (Nagel et al., 2004; Damm and Winklbauer, 2011). PDGF signaling also regulates cell polarization and the formation of cellular processes by mesendodermal cells in zebrafish, but apparently not their directional migration (Montero et al., 2003). In *Drosophila*, FGF regulates several mesoderm cell behaviors,

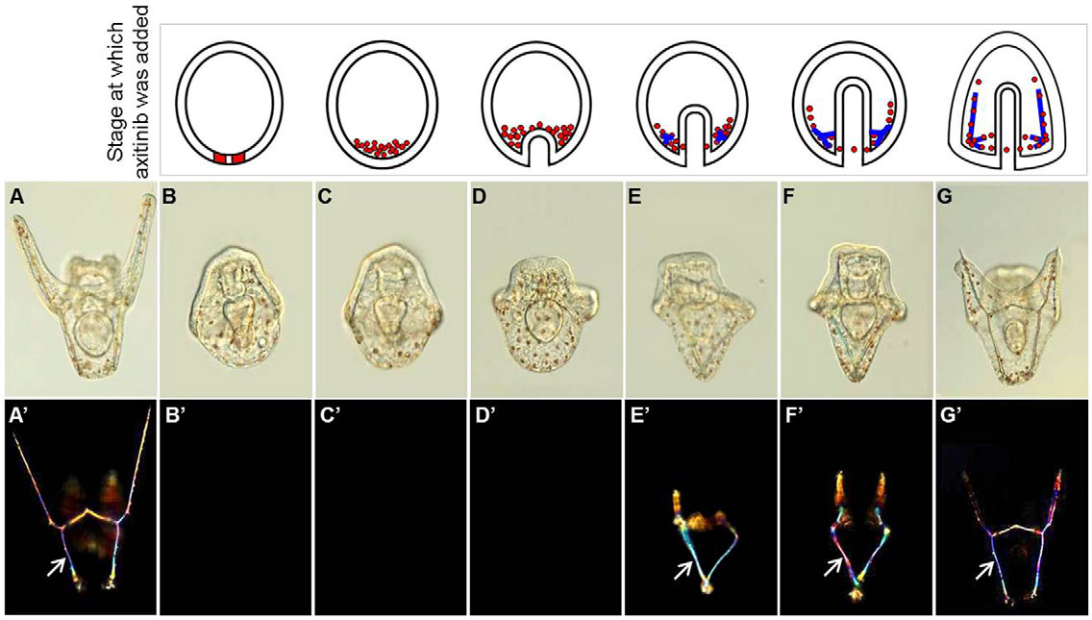

Fig. 11. VEGF signaling regulates biomineralization independently of its role in PMC guidance. DIC (A-G) and polarized light (A′-G′) images of a control embryo (**A**,**A′**), and embryos treated with axitinib at the hatched blastula (**B**,**B′**), mesenchyme blastula (**C**,**C′**), early gastrula (**D**,**D′**), mid-gastrula (**E**,**E′**), late gastrula (**F**,**F′**) or prism (**G**,**G′**) stages. Inhibition of VEGF signaling prior to the mid-gastrula stage completely blocks biomineralization (B′-D′), whereas VEGFR inhibition at or after mid-gastrula leads to the formation of truncated skeletal elements (E′-G′). Arrows (A′,E′-G′) indicate body rods. Diagrams indicate the stage at which axitinib was added to embryo cultures (PMCs are represented in red and skeletal elements in blue).

including EMT, intercalation, spreading, and attachment to the epithelium prior to migration (Wilson and Leptin, 2000; Winklbauer and Müller, 2011). In sea urchins, VEGF3 regulates the formation of cellular processes and directional migration. In contrast to mesodermal cells in *Drosophila* and *Xenopus*, however, the ingression and spreading of PMCs is independent of growth factor-mediated signaling. In addition, VEGF signaling is not required for PMC translocation or fusion, but only for guidance. We hypothesize that the effect of VEGF3 on the number and length of PMC filopodia is associated in some way with the defect in pathfinding, although the relationship is unclear.

In vertebrate endothelial cells, VEGF regulates filopodial extension and acts a chemoattractant to direct cell migration (Gerhardt et al., 2003; Gerhardt, 2008; Shamloo et al., 2008). These findings, and the observation that PMCs accumulate at ectopic sites of VEGF expression (Duloquin et al., 2007), indicate that VEGF3 functions as a chemoattractant in the sea urchin. Our finding that *Lv-vegf3* expression is initially confined to a ring of ectoderm at the vegetal pole of the blastula and subsequently resolves to the ectoderm overlying the VLCs might account for the observation that vegetal directional cues are established even before PMC ingression (Ettensohn and McClay, 1986) and for the gradual emergence of the two PMC clusters during gastrulation (Malinda et al., 1995; Gustafson and Wolpert, 1999). Our findings further suggest that VEGF3 signaling is required for the second phase of PMC migration, during which chains of PMCs extend from the VLCs towards the animal pole. At present, owing to embryo to embryo variability in the timing of VEGF3 expression in the animal hemisphere during late

Table 1. Distribution of phenotypes in axitinib wash-in experiments

	Stage at which axitinib was added															
	2-cell		Hatched blastula		Mesenchyme blastula		Early gastrula		Mid-gastrula		Late gastrula		Prism		DMSO control	
Phenotype	*n*	%	*n*	%	*n*	%	*n*	%	*n*	%	*n*	%	*n*	%	*n*	%
No skeleton	**202**	**100**	**228**	**100**	**206**	**99.0**	**148**	**63.2**	15	7.4	1	0.5	0	0	0	0
Tiny skeletal deposits (specks)	0	0	0	0	2	1.0	68	29.1	11	5.4	4	1.9	2	0.9	0	0
Branched skeletal rudiments	0	0	0	0	0	0	18	7.7	13	6.4	3	1.4	1	0.4	2	0.9
Extended rods, with prominent body and dorsoventral connecting rods	0	0	0	0	0	0	0	0	**163**	**80.3**	**171**	**82.2**	21	9.1	0	0
Short pluteus skeleton	0	0	0	0	0	0	0	0	1	0.5	29	13.9	**208**	**89.6**	11	5.1
Wild-type skeleton	0	0	0	0	0	0	0	0	0	0	0	0	0	0	**204**	**94**
Total	202	100	228	100	208	100	234	100	203	100	208	100	232	100	217	100

Bold type indicates the prevalent phenotype observed.

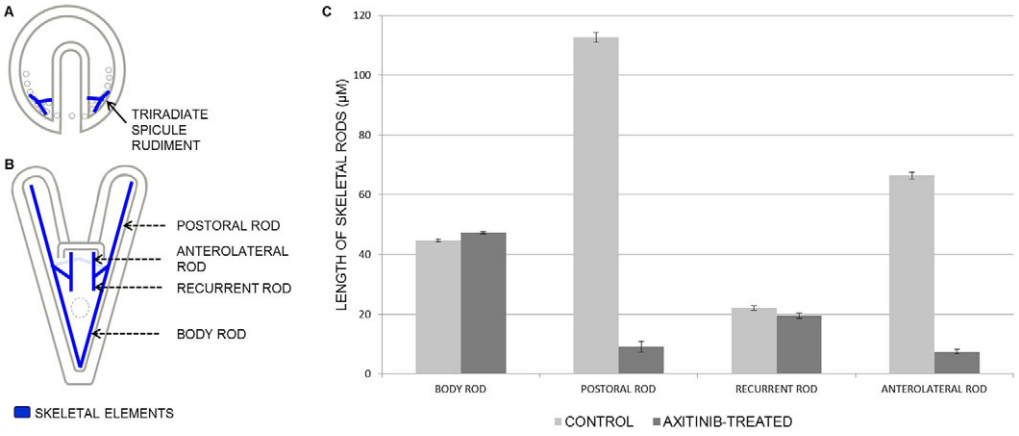

Fig. 12. VEGF signaling selectively inhibits the elongation of specific skeletal rods. (**A**,**B**) Schematics showing (A) the stage at which axitinib was added to embryo cultures and (B) the stage at which skeletal rods were measured using an ocular micrometer (skeletal elements are represented in blue). (**C**) The body rods and recurrent rods are of comparable length in control and axitinib-treated embryos, whereas the postoral and anterolateral rods are significantly shorter in axitinib-treated embryos. Error bars indicate s.e.m.

gastrulation, we do not know whether a VEGF3 concentration gradient directs this phase of PMC migration or whether VEGF3 signaling at the VLCs renders the cells competent to respond to other directional cues.

Although VEGF signaling is required for biomineral formation (Duloquin et al., 2007), it has been unclear whether this is a secondary effect of disrupting the normal pattern of PMC migration, which might prevent PMCs from receiving a different ectodermal signal. In this regard, the ectoderm overlying sites of skeletal rod growth is a local source of signaling factors other than VEGF3, including FGFA and WNT5. Using axitinib to inhibit VEGF signaling late in development, after PMC migration is largely complete, we have demonstrated an effect of VEGF signaling on biomineralization that is separable from its role in PMC patterning. It was shown previously that photoablation of the ectoderm overlying the postoral rods inhibits the growth of these rods, pointing to local, ectoderm-derived cues that regulate skeletogenesis at late embryonic stages (Ettensohn and Malinda, 1993). At the pluteus stage, *vegf3* and *vegfr-10-Ig* are expressed in the PMCs and ectoderm, respectively, at the tips of the elongating postoral and anterolateral rods (Fig. 1) (Duloquin et al., 2007). We have observed a striking selective inhibition of the elongation of exactly these rods when VEGF signaling is blocked late in development (Fig. 12). VEGF is not required, however, for the elongation of skeletal rods that form in the aboral region of the embryo.

The formation of biomineral is a complex, regulated process. It is possible that VEGF3 controls a feature of PMC motility and/or secretion that is required in the cell biology of biomineralization. Our findings, however, point to a more direct mechanism. PMC specification and differentiation are regulated by an elaborate transcriptional network (Rafiq et al., 2012). VEGF signaling controls the expression of numerous spicule matrix genes and other major protein components of the spicule (Fig. 13; supplementary material Table S3). The onset of expression of some of these genes precedes the expression of *vegfr-10-Ig* in the PMCs (Illies et al., 2002; Duloquin et al., 2007; Rafiq et al., 2012) and the expression of most genes was not fully blocked by inhibiting VEGF3, suggesting that VEGF signaling is not required for their initial activation but to maintain their expression. We favor the view that an initial, cell-autonomous phase of GRN deployment in the PMC lineage gives way to a later, signal-dependent phase during which local VEGF3 maintains the expression of a subset of biomineralization genes in specific regions of the PMC syncytium at levels compatible with skeletal growth. It is noteworthy that although the great majority of genes regulated by VEGF3 signaling have predicted or proven roles in biomineralization, not all genes encoding biomineralization proteins are regulated by VEGF signaling. For example, *p16* and members of the *msp130* gene family were not sensitive to VEGF signaling. Further analysis of the transcriptional regulatory control of these genes will be necessary to account for their differential responses to VEGF3.

Knapp et al. (Knapp et al., 2012) recently demonstrated concentration-dependent effects of recombinant VEGF3 on skeletal growth by cultured PMCs. Relatively high levels of VEGF3 favored growth in the a-axis (the formation of triradiate spicules), whereas lower levels of VEGF3 favored growth in the c-axis (the formation of linear rods that extend perpendicular to the plane of the triradiate spicule). These observations might be relevant to *in vivo* skeletogenesis, as *vegf3* mRNA appears to be expressed at higher levels during gastrulation, when the triradiate spicules are synthesized, whereas levels are lower at the prism and pluteus stages, when other skeletal rods (e.g. the postoral and anterolateral rods) extend in the direction of the c-axis.

Our data and those of Röttinger et al. (Röttinger et al., 2008) point to negative feedback mechanisms that regulate *fgfa* and *vegf3* in the ectoderm. We confirm that MO knockdown of FGFA enhances the expression of *fgfa* in the ectoderm and show a similar dependence of *vegf3* expression on VEGF3. Because the only known embryonically expressed VEGF receptor, VEGFR-10-Ig, is restricted to PMCs, the effect of VEGF3 on *vegf3* expression in the ectoderm is likely to be indirect. We report that the expression of *fgfa* in PMCs (but not in the ectoderm) is dependent on VEGF3, an effect that might be mediated directly by VEGFR-10-Ig. This provides evidence of cross-talk between these two pathways, which function synergistically in other systems (Tomanek et al., 2010). Cavalieri et al. (Cavalieri et al., 2011) showed that the tripartite motif-containing protein STRIM1 regulates the expression of *fgfa* in the ectoderm, but not in PMCs, highlighting the separate control of *fgfa* expression in these two tissues. STRIM1 also regulates *otp* in the ectoderm whereas VEGF3 and FGFA do not, suggesting that multiple pathways regulate gene expression in the ectoderm overlying the VLCs.

Our studies and those of Duloquin et al. (Duloquin et al., 2007) demonstrate a conserved role for VEGF3 in regulating PMC migration and differentiation in three species of sea urchin. Recent work suggests that evolutionary shifts in VEGF3 expression have been associated with changing patterns of skeletogenesis within the phylum (Morino et al., 2012). In contrast to the highly conserved function of VEGF3, the role of FGFA may vary among species, as this molecule has been implicated in PMC migration and skeletogenesis in *P. lividus* (Röttinger et al., 2008). In *L. variegatus*,

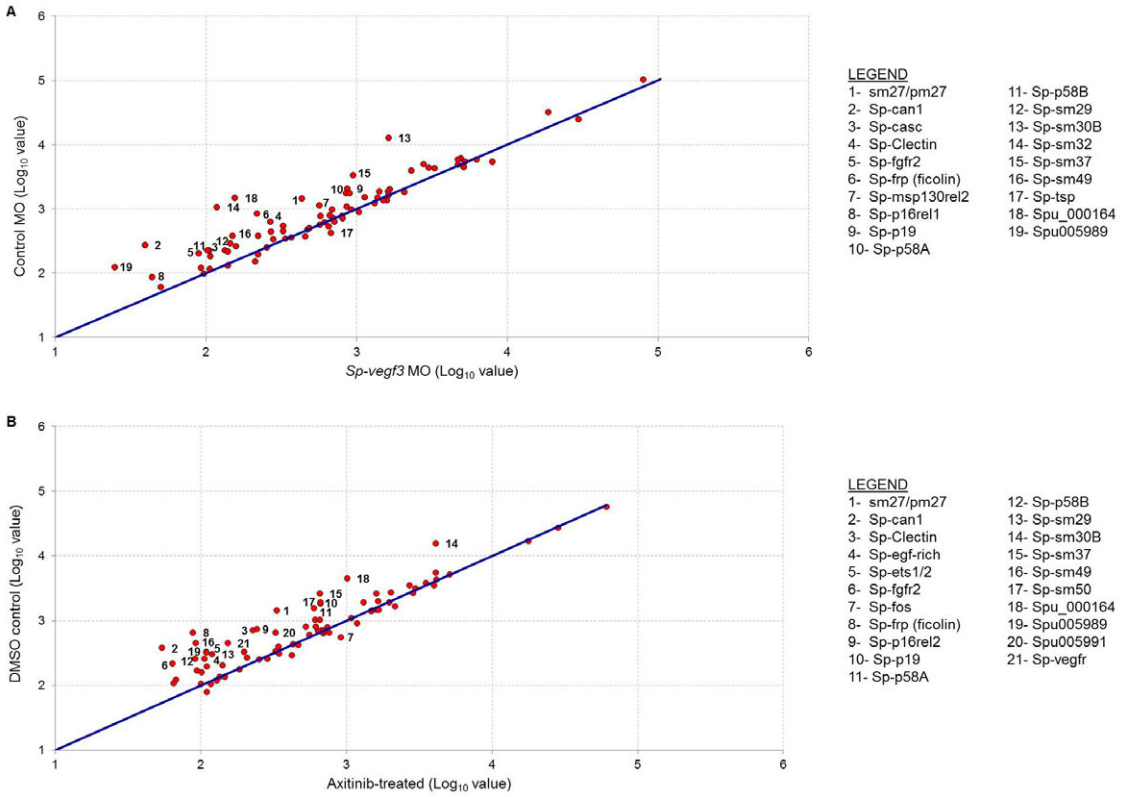

Fig. 13. VEGF signaling regulates the expression of genes in the PMC GRN. Analyses of changes in gene expression by the Nanostring nCounter system in (**A**) *Sp-vegf3* morphants and (**B**) axitinib-treated embryos reveal changes in the expression of many biomineralization-related genes. Legends list genes with changes of 50% or more between control and *Sp-vegf3* morphants or axitinib-treated embryos (*n*=3 trials for both axitinib-treated embryos and *Sp-vegf3* morphants).

we observed skeletal phenotypes similar to those reported by Röttinger and co-workers when we injected high concentrations of MO that also appeared to produce general toxic effects. At lower doses, all detectable FGF mRNA was mis-spliced (Fig. 2), but the overall morphology of the embryos was similar to that of controls, and we observed no effects on PMC migration and only subtle effects on skeletal growth. Thus, there might be technical issues that account for the reported differences in the phenotypes of FGF morphants in these two species, and the functions of both VEGF3 and FGFA might be conserved among echinoids.

The downstream components of the VEGF signaling pathway in PMCs are unknown. In other cell types, VEGF receptors signal via the MAPK and PI3 kinase pathways (Schlessinger, 2000), both of which are essential for skeletogenesis in the sea urchin embryo. Bradham et al. (Bradham et al., 2004) showed that inhibiting PI3K blocks the elongation of skeletal rods, but not PMC specification, cell migration, the extension of filopodia, cell fusion or skeletal initiation. The MAPK pathway, by contrast, regulates early PMC specification, thereby affecting all aspects of PMC morphogenesis (Fernandez-Serra et al., 2004; Röttinger et al., 2004). It has been suggested that MAPK signaling may regulate skeletogenesis by two distinct pathways: a Ras-independent pathway necessary for PMC ingression and a Ras-dependent pathway required for PMC migration and skeletogenesis (Fernandez-Serra et al., 2004; Röttinger et al., 2004). As the VEGF pathway does not regulate PMC ingression, it might function by a Ras/MAPK-dependent mechanism. Further research will be necessary to determine the molecular effectors of VEGF signaling in PMCs and the linkages between this pathway and the skeletogenic GRN.

Acknowledgements
We thank Kiran Rafiq for designing the Nanostring codeset.

Funding
This work was supported by National Science Foundation grants [IOS-0745875 and IOS-1021805 to C.A.E.].

Competing interests statement
The authors declare no competing financial interests.

Author contributions
A.A.-A. and C.A.E. designed the experiments. C.A.E. carried out microsurgical experiments and A.A.-A. carried out all other experiments. The manuscript was prepared by both A.A.-A. and C.A.E.

Supplementary material
Supplementary material available online at
http://dev.biologists.org/lookup/suppl/doi:10.1242/dev.100479/-/DC1

References

Adomako-Ankomah, A. and Ettensohn, C. A. (2011). P58-A and P58-B: novel proteins that mediate skeletogenesis in the sea urchin embryo. *Dev. Biol.* **353**, 81-93.
Armstrong, N., Hardin, J. and McClay, D. R. (1993). Cell-cell interactions regulate skeleton formation in the sea urchin embryo. *Development* **119**, 833-840.
Ataliotis, P., Symes, K., Chou, M. M., Ho, L. and Mercola, M. (1995). PDGF signalling is required for gastrulation of Xenopus laevis. *Development* **121**, 3099-3110.
Bhargava, P. and Robinson, M. O. (2011). Development of second-generation VEGFR tyrosine kinase inhibitors: current status. *Curr. Oncol. Rep.* **13**, 103-111.
Boulet, A. M. and Capecchi, M. R. (2012). Signaling by FGF4 and FGF8 is required for axial elongation of the mouse embryo. *Dev. Biol.* **371**, 235-245.
Bradham, C. A., Miranda, E. L., McClay, D. R. (2004). PI3K inhibitors block skeletogenesis but not patterning in sea urchin embryos. *Dev. Dyn.* **229**, 713-721.

Cavalieri, V., Spinelli, G. and Di Bernardo, M. (2003). Impairing Otp homeodomain function in oral ectoderm cells affects skeletogenesis in sea urchin embryos. *Dev. Biol.* **262**, 107-118.
Cavalieri, V., Guarcello, R. and Spinelli, G. (2011). Specific expression of a TRIM-containing factor in ectoderm cells affects the skeletal morphogenetic program of the sea urchin embryo. *Development* **138**, 4279-4290.
Cheers, M. S. and Ettensohn, C. A. (2004). Rapid microinjection of fertilized eggs. *Methods Cell Biol.* **74**, 287-310.
Chuai, M. and Weijer, C. J. (2009). Regulation of cell migration during chick gastrulation. *Curr. Opin. Genet. Dev.* **19**, 343-349.
Ciruna, B. and Rossant, J. (2001). FGF signaling regulates mesoderm cell fate specification and morphogenetic movement at the primitive streak. *Dev. Cell* **1**, 37-49.
Damm, E. W. and Winklbauer, R. (2011). PDGF-A controls mesoderm cell orientation and radial intercalation during Xenopus gastrulation. *Development* **138**, 565-575.
Di Bernardo, M., Castagnetti, S., Bellomonte, D., Oliveri, P., Melfi, R., Palla, F. and Spinelli, G. (1999). Spatially restricted expression of PlOtp, a *Paracentrotus lividus* orthopedia-related homeobox gene, is correlated with oral ectodermal patterning and skeletal morphogenesis in late-cleavage sea urchin embryos. *Development* **126**, 2171-2179.
Dorey, K. and Amaya, E. (2010). FGF signalling: diverse roles during early vertebrate embryogenesis. *Development* **137**, 3731-3742.
Duloquin, L., Lhomond, G. and Gache, C. (2007). Localized VEGF signaling from ectoderm to mesenchyme cells controls morphogenesis of the sea urchin embryo skeleton. *Development* **134**, 2293-2302.
Ettensohn, C. A. (1990). The regulation of primary mesenchyme cell patterning. *Dev. Biol.* **140**, 261-271.
Ettensohn, C. A. (2013). Encoding anatomy: Developmental gene regulatory networks and morphogenesis. *Genesis* **51**, 383-409.
Ettensohn, C. A. and Malinda, K. M. (1993). Size regulation and morphogenesis: a cellular analysis of skeletogenesis in the sea urchin embryo. *Development* **119**, 155-167.
Ettensohn, C. A. and McClay, D. R. (1986). The regulation of primary mesenchyme cell migration in the sea urchin embryo: transplantations of cells and latex beads. *Dev. Biol.* **117**, 380-391.
Ettensohn, C. A. and McClay, D. R. (1988). Cell lineage conversion in the sea urchin embryo. *Dev. Biol.* **125**, 396-409.
Fernandez-Serra, M., Consales, C., Livigni, A. and Arnone, M. I. (2004). Role of the ERK-mediated signaling pathway in mesenchyme formation and differentiation in the sea urchin embryo. *Dev. Biol.* **268**, 384-402.
Geiss, G. K., Bumgarner, R. E., Birditt, B., Dahl, T., Dowidar, N., Dunaway, D. L., Fell, H. P., Ferree, S., George, R. D., Grogan, T. et al. (2008). Direct multiplexed measurement of gene expression with color-coded probe pairs. *Nat. Biotechnol.* **26**, 317-325.
Gerhardt, H. (2008). VEGF and endothelial guidance in angiogenic sprouting. *Organogenesis* **4**, 241-246.
Gerhardt, H., Golding, M., Fruttiger, M., Ruhrberg, C., Lundkvist, A., Abramsson, A., Jeltsch, M., Mitchell, C., Alitalo, K., Shima, D. et al. (2003). VEGF guides angiogenic sprouting utilizing endothelial tip cell filopodia. *J. Cell Biol.* **161**, 1163-1177.
Guss, K. A. and Ettensohn, C. A. (1997). Skeletal morphogenesis in the sea urchin embryo: regulation of primary mesenchyme gene expression and skeletal rod growth by ectoderm-derived cues. *Development* **124**, 1899-1908.
Gustafson, T. and Wolpert, L. (1999). Studies on the cellular basis of morphogenesis in the sea urchin embryo. Directed movements of primary mesenchyme cells in normal and vegetalized larvae. *Exp. Cell Res.* **253**, 288-295.
Hardin, J., Coffman, J. A., Black, S. D. and McClay, D. R. (1992). Commitment along the dorsoventral axis of the sea urchin embryo is altered in response to NiCl2. *Development* **116**, 671-685.
Hodor, P. G. and Ettensohn, C. A. (2008). Mesenchymal cell fusion in the sea urchin embryo. *Methods Mol. Biol.* **475**, 315-334.
Hodor, P. G., Illies, M. R., Broadley, S. and Ettensohn, C. A. (2000). Cell-substrate interactions during sea urchin gastrulation: migrating primary mesenchyme cells interact with and align extracellular matrix fibers that contain ECM3, a molecule with NG2-like and multiple calcium-binding domains. *Dev. Biol.* **222**, 181-194.
Hogan, B. L. (1999). Morphogenesis. *Cell* **96**, 225-233.
Hu-Lowe, D. D., Zou, H. Y., Grazzini, M. L., Hallin, M. E., Wickman, G. R., Amundson, K., Chen, J. H., Rewolinski, D. A., Yamazaki, S., Wu, E. Y. et al. (2008). Nonclinical antiangiogenesis and antitumor activities of axitinib (AG-013736), an oral, potent, and selective inhibitor of vascular endothelial growth factor receptor tyrosine kinases 1, 2, 3. *Clin. Cancer Res.* **14**, 7272-7283.
Illies, M. R., Peeler, M. T., Dechtiaruk, A. M. and Ettensohn, C. A. (2002). Identification and developmental expression of new biomineralization proteins in the sea urchin Strongylocentrotus purpuratus. *Dev. Genes Evol.* **212**, 419-431.
Kadam, S., McMahon, A., Tzou, P. and Stathopoulos, A. (2009). FGF ligands in Drosophila have distinct activities required to support cell migration and differentiation. *Development* **136**, 739-747.
Knapp, R. T., Wu, C. H., Mobilia, K. C. and Joester, D. (2012). Recombinant sea urchin vascular endothelial growth factor directs single-crystal growth and branching in vitro. *J. Am. Chem. Soc.* **134**, 17908-17911.
Lapraz, F., Röttinger, E., Duboc, V., Range, R., Duloquin, L., Walton, K., Wu, S.-Y., Bradham, C., Loza, M. A., Hibino, T. et al. (2006). RTK and TGF-β signaling pathways genes in the sea urchin genome. *Dev. Biol.* **300**, 132-152.
Lepage, T., Sardet, C. and Gache, C. (1992). Spatial expression of the hatching enzyme gene in the sea urchin embryo. *Dev. Biol.* **150**, 23-32.
Lunn, J. S., Fishwick, K. J., Halley, P. A. and Storey, K. G. (2007). A spatial and temporal map of FGF/Erk1/2 activity and response repertoires in the early chick embryo. *Dev. Biol.* **302**, 536-552.
Malinda, K. M., Fisher, G. W. and Ettensohn, C. A. (1995). Four-dimensional microscopic analysis of the filopodial behavior of primary mesenchyme cells during gastrulation in the sea urchin embryo. *Dev. Biol.* **172**, 552-566.
McMahon, A., Reeves, G. T., Supatto, W. and Stathopoulos, A. (2010). Mesoderm migration in Drosophila is a multi-step process requiring FGF signaling and integrin activity. *Development* **137**, 2167-2175.
Montero, J. A., Kilian, B., Chan, J., Bayliss, P. E. and Heisenberg, C. P. (2003). Phosphoinositide 3-kinase is required for process outgrowth and cell polarization of gastrulating mesendodermal cells. *Curr. Biol.* **13**, 1279-1289.
Morino, Y., Koga, H., Tachibana, K., Shoguchi, E., Kiyomoto, M. and Wada, H. (2012). Heterochronic activation of VEGF signaling and the evolution of the skeleton in echinoderm pluteus larvae. *Evol. Dev.* **14**, 428-436.
Nagel, M., Tahinci, E., Symes, K. and Winklbauer, R. (2004). Guidance of mesoderm cell migration in the Xenopus gastrula requires PDGF signaling. *Development* **131**, 2727-2736.
Rafiq, K., Cheers, M. S. and Ettensohn, C. A. (2012). The genomic regulatory control of skeletal morphogenesis in the sea urchin. *Development* **139**, 579-590.
Reim, I., Hollfelder, D., Ismat, A. and Frasch, M. (2012). The FGF8-related signals Pyramus and Thisbe promote pathfinding, substrate adhesion, and survival of migrating longitudinal gut muscle founder cells. *Dev. Biol.* **368**, 28-43.
Röttinger, E., Besnardeau, L. and Lepage, T. (2004). A Raf/MEK/ERK signaling pathway is required for development of the sea urchin embryo micromere lineage through phosphorylation of the transcription factor Ets. *Development* **131**, 1075-1087.
Röttinger, E., Saudemont, A., Duboc, V., Besnardeau, L., McClay, D. and Lepage, T. (2008). FGF signals guide migration of mesenchymal cells, control skeletal morphogenesis [corrected] and regulate gastrulation during sea urchin development. *Development* **135**, 353-365.
Schlessinger, J. (2000). Cell signaling by receptor tyrosine kinases. *Cell* **103**, 211-225.
Shamloo, A., Ma, N., Poo, M. M., Sohn, L. L. and Heilshorn, S. C. (2008). Endothelial cell polarization and chemotaxis in a microfluidic device. *Lab Chip* **8**, 1292-1299.
Sharma, T. and Ettensohn, C. A. (2010). Activation of the skeletogenic gene regulatory network in the early sea urchin embryo. *Development* **137**, 1149-1157.
Sun, X., Meyers, E. N., Lewandoski, M. and Martin, G. R. (1999). Targeted disruption of Fgf8 causes failure of cell migration in the gastrulating mouse embryo. *Genes Dev.* **13**, 1834-1846.
Thompson, J. D., Higgins, D. G. and Gibson, T. J. (1994). CLUSTAL W: improving the sensitivity of progressive multiple sequence alignment through sequence weighting, position-specific gap penalties and weight matrix choice. *Nucleic Acids Res.* **22**, 4673-4680.
Tomanek, R. J., Christensen, L. P., Simons, M., Murakami, M., Zheng, W. and Schatteman, G. C. (2010). Embryonic coronary vasculogenesis and angiogenesis are regulated by interactions between multiple FGFs and VEGF and are influenced by mesenchymal stem cells. *Dev. Dyn.* **239**, 3182-3191.
Voronina, E. and Wessel, G. M. (2001). Apoptosis in sea urchin oocytes, eggs, and early embryos. *Mol. Reprod. Dev.* **60**, 553-561.
Wilson, R. and Leptin, M. (2000). Fibroblast growth factor receptor-dependent morphogenesis of the Drosophila mesoderm. *Philos. Trans. R. Soc. B* **355**, 891-895.
Wilt, F. H. and Ettensohn, C. A. (2007). Morphogeneisis and biomineralization of the sea urchin larval endoskeleton. In *Handbook of Biomineralization* (ed. E. Bauerlein), pp. 183-210. Weinheim: Wiley-VCH.
Winklbauer, R. and Müller, H. A. (2011). Mesoderm layer formation in Xenopus and Drosophila gastrulation. *Phys. Biol.* **8**, 045001.
Wu, M. Y. and Hill, C. S. (2009). Tgf-beta superfamily signaling in embryonic development and homeostasis. *Dev. Cell* **16**, 329-343.
Yang, X., Dormann, D., Münsterberg, A. E. and Weijer, C. J. (2002). Cell movement patterns during gastrulation in the chick are controlled by positive and negative chemotaxis mediated by FGF4 and FGF8. *Dev. Cell* **3**, 425-437.
Yang, X., Chrisman, H. and Weijer, C. J. (2008). PDGF signalling controls the migration of mesoderm cells during chick gastrulation by regulating N-cadherin expression. *Development* **135**, 3521-3530.